Journal for ImmunoTherapy of Cancer

Preclinical characterization and clinical translation of pharmacodynamic markers for MK-5890: a human CD27 activating antibody for cancer immunotherapy

Lars Guelen,[1] Thierry O Fischmann,[2] Jerelyn Wong,[3] Smita Mauze,[3] Marco Guadagnoli,[1] Nikolina Bąbała,[4] Jozef Wagenaars,[1] Veronica Juan,[3] David Rosen,[3] Winnie Prosise,[2] Maurice Habraken,[1] Imke Lodewijks,[1] Danling Gu,[3] Judith Stammen-Vogelzangs,[1] Ying Yu,[3] Jeanne Baker,[3] David Lutje Hulsik,[1] Lilian Driessen-Engels,[1] Dan Malashock,[3] Joost Kreijtz,[1] Astrid Bertens,[1] Evert de Vries,[4] Astrid Bovens,[4] Arne Bramer,[1] Yiwei Zhang,[5] Richard Wnek,[2] Sean Troth,[6] Elliot Chartash,[5] Konstantin Dobrenkov,[5] Svetlana Sadekova,[3] Andrea van Elsas,[1] Jason K Cheung,[7] Laurence Fayadat-Dilman,[3] Jannie Borst,[4] Amy M Beebe ,[3] Hans Van Eenennaam[1]

To cite: Guelen L, Fischmann TO, Wong J, *et al*. Preclinical characterization and clinical translation of pharmacodynamic markers for MK-5890: a human CD27 activating antibody for cancer immunotherapy. *Journal for ImmunoTherapy of Cancer* 2022;**10**:e005049. doi:10.1136/jitc-2022-005049

► Additional supplemental material is published online only. To view, please visit the journal online (http://dx.doi.org/10.1136/jitc-2022-005049).

LG and TOF are joint first authors.

AMB and HVE are joint senior authors.

Accepted 23 August 2022

For numbered affiliations see end of article.

Correspondence to
Dr Amy M Beebe;
amy.beebe@merck.com

ABSTRACT

Background Immune checkpoint inhibitors (ICI) have radically changed cancer therapy, but most patients with cancer are unresponsive or relapse after treatment. MK-5890 is a CD27 agonist antibody intended to complement ICI therapy. CD27 is a member of the tumor necrosis factor receptor superfamily that plays a critical role in promoting responses of T cells, B cells and NK cells.

Methods Anti-CD27 antibodies were generated and selected for agonist activity using NF-κB luciferase reporter assays. Antibodies were humanized and characterized for agonism using in vitro T-cell proliferation assays. The epitope recognized on CD27 by MK-5890 was established by X-ray crystallography. Anti-tumor activity was evaluated in a human CD27 knock-in mouse. Preclinical safety was tested in rhesus monkeys. Pharmacodynamic properties were examined in mouse, rhesus monkeys and a phase 1 dose escalation clinical study in patients with cancer.

Results Humanized anti-CD27 antibody MK-5890 (hIgG1) was shown to bind human CD27 on the cell surface with sub-nanomolar potency and to partially block binding to its ligand, CD70. Crystallization studies revealed that MK-5890 binds to a unique epitope in the cysteine-rich domain 1 (CRD1). MK-5890 activated CD27 expressed on 293T NF-κB luciferase reporter cells and, conditional on CD3 stimulation, in purified CD8+ T cells without the requirement of crosslinking. Functional Fc-receptor interaction was required to activate CD8+ T cells in an ex vivo tumor explant system and to induce antitumor efficacy in syngeneic murine subcutaneous tumor models. MK-5890 had monotherapy efficacy in these models and enhanced efficacy of PD-1 blockade. MK-5890 reduced in an isotype-dependent and dose-dependent manner circulating, but not tumor-infiltrating T-cell numbers in these mouse models. In rhesus monkey and human patients, reduction in circulating T cells was transient and less pronounced than in mouse. MK-5890 induced transient elevation of chemokines MCP-1, MIP-1α, and MIP-1β in the serum of mice, rhesus monkeys and patients with cancer. MK-5890 was well tolerated in rhesus monkeys and systemic exposure to MK-5890 was associated with CD27 occupancy at all doses.

Conclusions MK-5890 is a novel CD27 agonistic antibody with the potential to complement the activity of PD-1 checkpoint inhibition in cancer immunotherapy and is currently undergoing clinical evaluation.

INTRODUCTION

The activity of immune cells that are engaged in an antitumor immune response is tightly orchestrated by a broad array of costimulatory and coinhibitory receptors. Over the past decade, monoclonal antibodies that block the coinhibitory receptors cytotoxic T lymphocyte-associated protein-4 and programmed cell death protein 1 (PD-1), and its ligand PD-L1, collectively referred to as immune checkpoint inhibitors (ICIs), have transformed cancer treatment. However, patients are often refractory to or relapse after ICI targeted therapies. A complementary approach is the use of antibodies that can activate costimulatory receptors on immune cells. Because of its function and expression pattern, TNFRSF7, also known as CD27, is a candidate target for the development of agonist antibodies that might shape the next generation of immunotherapy strategies.

CD27 is constitutively expressed on most T cells, including naïve CD4+ and CD8+ T cells, germinal center and memory B cells, and a subset of NK cells.[1 2] Its ligand, CD70, shows tightly orchestrated, transient expression on T cells, B cells, NK cells and dendritic cells (DC) on their activation by pathogen-derived or immune cell-derived stimuli.[3] Engagement of the CD27/CD70 axis promotes CD8+ and CD4+ T cell responses by promoting the survival of clonally expanding T cells in lymphoid organs and of effector T cells in non-lymphoid organs.[4 5] CD27 complements CD28 in this aspect.[4] CD27/CD70 costimulation promotes T helper-1 differentiation of CD4+ T cells[6 7] and cytotoxic T lymphocyte (CTL) effector differentiation of CD8+ T cells.[8 9] The 'help' for CTL priming, effector and memory differentiation that CD4+ T cells provide, relies to a large extent on interaction between CD70 on DC and CD27 on CD8+ T cells.[9–11] CD4+ T cell help promotes clonal expansion and effector differentiation of CD8+ T cells resulting in CTLs with enhanced motility and migratory capabilities that avoid dysfunction and exhaustion.[9 12] In the absence of CD4+ T cell help in a therapeutic vaccination model, combined CD27 agonism and PD-1 blockade recapitulated the effects of CD4+ T cell help and resulted in full tumor control.[13]

Sakanishi and Yagita demonstrated that treatment with an agonist antibody directed at mouse CD27 resulted in an effective antitumor response.[14] The development of agonist antibodies targeting CD27 and other TNFRSF members has proven to be complex. Many factors may influence the ability of an antibody to act as an agonist, including binding epitope, affinity, antibody and target valency, degree of receptor occupancy, and interaction with Fcγ receptors (FcγRs). Varlilumab (CDX-1127), an anti-human CD27 antibody demonstrated to induce tumor rejection in human CD27-transgenic mice, was shown to require antibody cross-linking to trigger T-cell activation in combination with T-cell receptor (TCR) costimulation in vitro.[15 16] Here, we describe the preclinical characterization of MK-5890, an anti-human CD27 agonist antibody that triggers activation of CD27 and costimulates CD8+ T cells in vitro without the need for antibody cross-linking. MK-5890 demonstrates robust efficacy as a monotherapy in syngeneic tumor models and potentiates the effect of PD-1 blockade on tumor outgrowth. MK-5890 was well tolerated in rhesus monkeys and, at present, is under clinical development for the treatment of cancer.

METHODS

Generation of MK-5890

Female BALB/c mice were immunized using cDNA encoding human (hu) CD27 and hybridomas were generated as described in online supplemental additional file 1. Antibodies that were selected based on binding to human and rhesus monkey CD27, cross-blocking of hCD27.15[17] binding to CD27 and bioactivity in engineered and primary cell assays were humanized by complementarity-determining region (CDR) grafting technology using structure guided design. Mouse variable heavy chain (VH) and variable light chain (VL) variable domain sequences were compared with and grafted onto a human IgG1 antibody-germline sequence. Based on structural considerations, framework substitutions were incorporated to maintain binding of MK-5890 equivalent to its parental antibody (hCD27.131A).[18]

Additional antibodies

To support the choice of Fc domain, a hIgG2 version of the hIgG1 MK-5890 was made (MK-5890 hIgG2), as well as chimeric versions of the parental mouse clone hCD27.131A engineered with Fc mutations, hCD27.131A hIgG2 N297A or hCD27.131A mIgG1 D265A. An analog of anti-CD27 fully human IgG1 antibody varlilumab (to be referred to as varlilumab) was made in-house based on published patented sequences (US9169325B2).[19] Anti-PD-1 antibodies used were pembrolizumab and muDX400, a mouse IgG1 D265A anti-mouse PD-1 antibody.[20] A murinized IgG2a version of rat-anti-mouse GITR agonist antibody DTA-1 generated on the basis of published sequences has been previously described.[21]

Human CD27 Knock-In mice

Generation and characterization of human CD27 knock-in mice (huCD27 KI; B6.Cg-Cd27$^{tm1(Cd27)Jbo}$/Tac) is described in online supplemental additional file 2.

Blood and tissue sources

Blood from human healthy volunteers, fresh human tumor tissues and blood from rhesus monkeys was sourced as described in online supplemental additional file 1.

CD27 binding by cell-based ELISA and flow cytometry

Binding of anti-CD27 antibodies to CHO-K1 cells vs CHO-K1 cells engineered to express human, rhesus monkey, or mouse CD27 or mouse/human CD27 domain exchange mutants was determined by cell-based ELISA and flow cytometry (online supplemental additional file 1). Binding to primary human or rhesus monkey peripheral blood T cells was assessed by flow cytometry on fresh whole blood (online supplemental additional file 1).

Antibody affinity measurement

A surface plasmon resonance based (SPR) assay was used to determine bivalent binding kinetics of anti-CD27 antibodies for human CD27 and rhesus monkey CD27 (online supplemental additional file 1).

Blockade of CD27-CD70 interaction

CHO-huCD27 cells and anti-CD27 antibodies, titrated 1:5 from 20 µg/mL, were incubated for 1 hour on ice, followed by addition of biotinylated soluble huCD70 protein at 2.5 µg/mL. After 1 hour, cells were washed and incubated for 45 min on ice with streptavidin-BV421 (Biolegend Cat#405225) for detection, followed by analysis on a Novocyte 3000 flow cytometer using the 405 nm laser.

Structure determination of the CD27-MK-5890 Fab complex

Details of Fab-CD27 complex generation, crystallization and structure determination can be found in online supplemental additional file 1.

NFκB-luciferase reporter assay

HEK293FT human embryonic kidney cells containing a NF-κB luciferase reporter were transiently transfected with a cDNA vector encoding human or rhesus monkey CD27. Approximately 16 hours later, cells were replated in Opti-MEM (Life Technologies) at 5000–10 000 cells per well into 96-well clear-bottom luminescence plates (Corning). Cells were allowed to rest and adhere for 30 to 180 min at 37°C before stimulation in triplicate with dilutions of anti-huCD27 antibodies and incubation for 16–20 hours at 37°C. NF-κB activation was assessed using Bright-Glo (Promega) according to manufacturer's recommendations. Plates were analyzed on a Luminescence plate reader (Molecular Devices). Fold changes in luminescence between antibody and no antibody conditions were calculated using GraphPad Prism software.

Costimulation of primary T cells

Human and rhesus CD8+ and CD4+ T cells were isolated from blood using commercially available methods (online supplemental additional file 1).

Enriched CD8+ cells were re-suspended to 7.5×10^5 cells/mL in DMEM-F12, 5% heat inactivated human serum, 50 µM 2-mercaptoethanol, 100 U/mL penicillin, and 100 µg/mL streptomycin. Cells were cultured for 3 days at 1.5×10^5/well in the presence of a sub-optimal dose of 0.025–0.05 µg/mL anti-CD3 mAb (clone OKT3, BioLegend) and 1 µg/mL anti-CD28 mAb (clone 15E8, Millipore) with at most 15 µg/mL soluble or 1 µL bead-bound anti-CD27 antibody (details in online supplemental additional file 1) in a flat-bottom 96-well plate. Enriched CD4+ cells were re-suspended, plated and cultured as described above with bead-bound anti-CD27 Abs (1:3 titration from 1 µL to 0.0041 µL), in the presence of a sub-optimal concentration of anti-CD3 mAb (0.3 µg/mL clone OKT3 for human; 0.625–1.25 ng/mL clone FN18, MRL for rhesus monkey) and anti-CD28 mAb (1 µg/mL clone 15E8 for human; 1 µg/mL clone CD28.2, BD Biosciences for rhesus monkey).

Following stimulation, cells were washed with PBS and stained with a fixable viability dye (eBioscience) for 30 min at 4°C, washed and blocked with TruStain FcX (BioLegend). Cells were incubated with phenotyping antibodies (online supplemental additional file 1, table 2) for 30 min at 4°C before being washed, fixed, and acquired on the BD LSRII or Fortessa flow cytometer (BD Biosciences). Activation of T cells was measured using the surface markers CD25 and CD69.

Induction of IFNγ in primary human tumor culture assays

Fresh non-small cell lung cancer (NSCLC) tumor tissues were processed into single cells suspensions by fine cutting with a scalpel, followed by a 30 min incubation at 37°C in digestion media composed of 10 mL DMEM with 0.5 mg/mL collagenase type I, and 400 U/mL DNase I. Single cells were separated from undigested material with a 70 µM strainer and washed. If cell viability was less than 30%, a Ficoll-density gradient separation was performed to enrich live cells. A total of 0.1×10^6 tumor digested cells per well were cultured in 96-well round-bottom plates and stimulated with 10 ng/mL soluble anti-CD3 (BioLegend, clone OKT3) in the presence of indicated concentration of MK-5890 or Fc mutant hCD27.131A mIgG1 D265A, 10 µg/mL pembrolizumab, or 20 µg/mL IgG1 isotype control mAb. The supernatants were collected on day 6 and IFNγ was measured using a human IFNγ tissue culture kit (Meso Scale Discovery).

Syngeneic mouse tumor models

Female huCD27 KI mice at 8–12 weeks of age were inoculated subcutaneously in the lower right flank with either 1×10^6 MC38 mouse colon adenocarcinoma cells or 0.5×10^6 mouse MB49 urothelial carcinoma cells (online supplemental additional file 1). When average tumor volume reached approximately 90 mm^3, groups of 10 mice per condition were dosed intraperitoneally every 3–4 days with anti-CD27 antibody (3–7 doses) and/or with muDX400 (4 doses). Tumor width and length were measured twice a week and tumor volume was calculated as $0.5\times length\times width^2$.

Toxicity study in rhesus monkey

The safety of MK-5890 was assessed in a GLP-compliant 4-week intravenous toxicity study in rhesus monkeys with a 12-week treatment-free period. Rhesus monkeys were assigned to four groups of five females and five males each and administered once weekly (on study days 1, 8, 15, and 22) intravenous doses (0, 0.1, 3, or 30 mg/kg/week) of MK-5890 for 4 weeks.

Three animals/sex/group were designated for end-of-dosing necropsy on study day 25 (3 days after the last dose). An additional two animals/sex/group were designated for recovery and euthanized after a 12-week treatment free period.

Animals were monitored throughout the study and samples were collected at indicated times and analyzed for MK-5890 concentration, CD27 target engagement, anti-MK-5890 antibody, cytokines and immunophenotyping (online supplemental additional file 1).

Phase I dose escalation study

The safety, pharmacokinetics and pharmacodynamics of MK-5890 as monotherapy and in combination with pembrolizumab was assessed in participants with advanced solid tumors (NCT03396445). Samples were collected and analyzed for MK-5890 concentration, CD27 target engagement, cytokines and immunophenotyping (online supplemental additional file 1).

Table 1 Binding characteristics of MK-5890 and varlilumab

Antibody	Target	Affinity by surface plasmon resonance (Biacore)			Flow cytometry EC_{50}±SD (nM)		CHO-ELISA EC_{50}±SD (nM)
		k_a ($M^{-1}s^{-1}$)	k_d (s^{-1})	K_D ± SD (nM)	CD8+ T	CD4+ T	
MK-5890	Human CD27	2.2×10^{5}	1.1×10^{-3}	5.1±0.1	0.30±0.07	0.32±0.07	0.072±0.013
	Rhesus CD27	2.3×10^{5}	1.0×10^{-3}	4.3±0.2	0.22±0.08	0.17±0.07	0.054±0.005
varlilumab	Human CD27	1.9×10^{5}	1.2×10^{-4}	0.63±0.02	1.30±0.60	1.54±0.80	0.325±0.068
	Rhesus CD27	2.3×10^{5}	2.2×10^{-4}	0.97±0.01	1.92±3.81	1.58±0.29	0.193±0.063

Binding affinity of anti-CD27 Abs was determined using Biacore instrumentation with human CD27-IgG and rhesus monkey CD27-IgG fusion proteins captured on the chip. Binding of anti-CD27 Abs to human and rhesus monkey peripheral blood mononuclear T cells was determined based on mean fluorescence intensity using flow cytometry. Binding of anti-CD27 Abs to CHO cells expressing human or rhesus monkey CD27 was assessed using an ELISA. k_a=association rate constant; k_d=dissociation rate constant; K_D=equilibrium dissociation constant; M=molar; nM=nanomolar; s=seconds; SD=SD deviation. CHO=Chinese hamster ovary, EC_{50}=half-maximal effective concentration(s)

RESULTS

Binding to human and rhesus monkey CD27

Anti-CD27 antibodies were characterized for binding to human and rhesus monkey CD27. MK-5890 bound human and rhesus monkey CD27 approximately fourfold better than varlilumab in a CHO-CD27 cell-based ELISA and by flow cytometry using peripheral blood T cells (table 1). However, comparison of binding affinity determined by SPR using a CD27-coated CM5 chip showed the opposite relationship. An approximately 8-fold lower K_D for varlilumab vs MK-5890 was primarily due to a tenfold faster off-rate for MK-5890. Binding of MK-5890 to human and rhesus monkey CD27 was comparable by all three methods (table 1). As shown in figure 1A, MK-5890 partially blocked the binding of soluble CD70 to membrane expressed CD27 with an IC50 of 0.24 nM, while varlilumab fully blocked with an IC50 of 2.85 nM.

Structural characterization of MK-5890 binding to CD27 by X-ray crystallography

To provide a structural basis for the binding of MK-5890 to human CD27, complexes of MK-5890 Fab with a CD27 construct encompassing most of the extracellular region were generated and crystallized, and the atomic structure was determined by X-ray crystallography. The Fab is mostly ordered in the structure, except for the C-terminal residues of both the heavy and light chain, as well as loop Lys132-Gly136 that connects two strands of the CH1 beta sheet. CD27 is also mostly ordered, except for the N-terminal and C-terminal residues (beyond residues 121). MK-5890 Fab overall structure is, as expected, typical of an antibody Fab: compared with the Fab used in the molecular replacement, the root-mean-square deviations values for Cα's are 0.9 Å, 1.1 Å, 0.4 Å and 0.5 Å for the VL, VH, constant light (CL) and CH1 regions, respectively. The elbow angle of 157° is well within the typical range of values. For the CD27 antigen, the ordered region closely matches the boundaries set by the first and last cysteine implicated in a disulfide bridge, Cys 27 and Cys 120, underlining the importance of the disulfide covalent bridges for the CD27 extracellular domain structural integrity.

MK-5890 binds at one end of the cylindrical shape of CD27 (figure 1B), which is CRD1. The long axis of this cylinder is strongly slanted relative to the axis of the superposition relating the VL and VH domains. The formation of the complex buries 649 $Å^2$ and 543 $Å^2$ of antigen and antibody surfaces, respectively (calculation with PISA). All three CDRs from both variable regions are involved in interactions with CD27 with the epitope involving residues from three segments: Pro28 to His31, Lys37 to Leu38 and Asp54 to Lys58 (figure 1C). The latter has the sequence Asp-Gln-His-Arg-Lys, which are all amino acids with polar side chains that form a complex network of polar interactions with the antibody. The two consecutive CD27 residues His56 and Arg57 are involved in salt bridges, with VH Asp101 and VL Asp49 in a bidentate interaction, respectively (note: a 3.2 Å cut-off distance is used for salt bridges, 3.3 Å for H-bonds, and 4.0 Å for other interactions). The epitope loop 54–58 is also involved in an additional 8 H-bonds. The Gln55 side-chain plays a key role as it fits in a groove between the heavy chain CDR2 and CDR3, its side-chain amide sharing a total of 5 H-bonds with the paratope, two of those with Fab main-chain atoms. Finally, another key polar interaction is present outside this loop, between the main-chain N atom of Glu29, with Tyr 31 from the light chain CDR1.

Heckel *et al* recently provided in silico docking analysis of hCD27.15 and other agonistic CD27 antibodies.[16] Since MK-5890 was selected based on its capacity to block the binding of hCD27.15 to CD27 we compared the MK-5890 binding site to the hCD27.15 epitope predicted by in silico modeling. Although not identical binding regions were found, both MK-5890 and hCD27.15 displayed overlapping binding to the external-facing residues of CRD1 and displayed perpendicular binding to CD27. The recent description of the CD27:CD70 trimeric complex[22] allowed comparison between MK-5890 bound to CD27 vs CD27 bound to CD70. As illustrated in figure 1D, the CD27 fold between MK-5890 complexed to CD27 vs CD27:CD70 complex (PDB 7KXO) is overall maintained. Similar observations were made comparing CD27 folds complexed with antagonistic antibodies M2177 (PBD

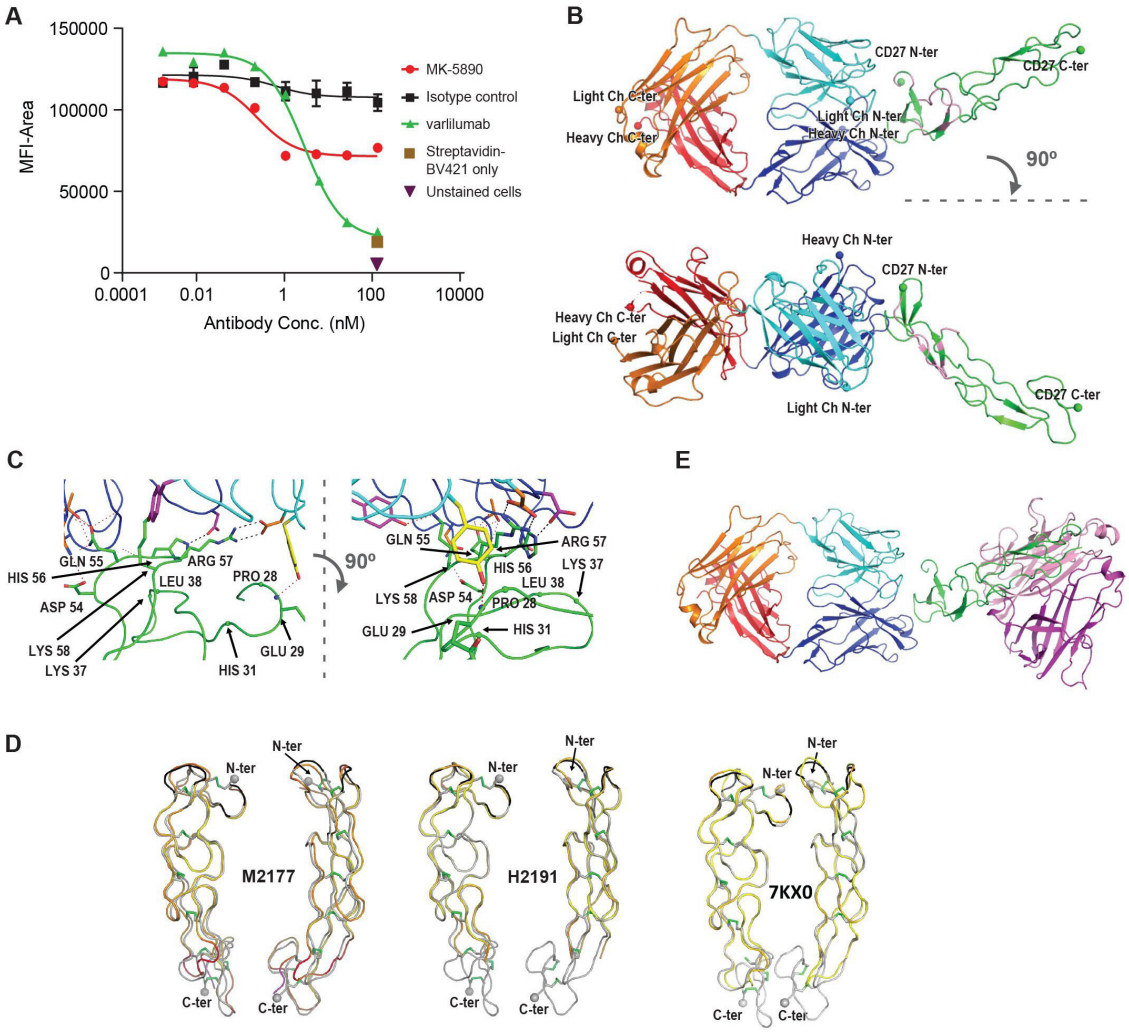

Figure 1 Binding epitope of MK-5890. (A) Binding of biotinylated soluble hCD70 protein to CHO-hCD27 cells that were preincubated with MK-5890 (red circle) or varlilumab (green triangle) or human IgG1 isotype control (black square) for 1 hour on ice. CD70 binding was measured by flow cytometry after incubation with streptavidin-BV421. (B) Overall view of the MK-5890 Fab-CD27 complex. Each protein backbone is represented as a cartoon. The positions of the ordered N-terminal and C-terminal residues Cα are marked with a sphere and labeled for each chain. The Fab VL, VH, CL, and CH domains, and the antigen, are colored cyan, blue, orange, red, and green, respectively, with one exception: CD27 residues part of the H2191 Fab's epitope are colored pink. Views on top and bottom are identical but for a 90° rotation around a horizontal axis and are chosen so that the axis of the superposition of the VL and VH domains is approximately horizontal. All figures were prepared with PyMol. (C) MK-5890 Fab-CD27 interface and key interactions. Color scheme as in B. The protein fragments are schematized as ribbons; all side-chains involved in polar interactions across the Fab-CD27 interface are shown as sticks. The Cα positions of CD27 epitope residues involved only in non-polar interactions are marked with a sphere, the epitope being defined as any antigen residue with at least one atom within 4 Å of the paratope. Salt bridges and H-bonds across the interface are represented with black and red dashes, respectively. All epitope residues are labeled. The methyls of CD27, Fab framework, light chain backbone, heavy chain backbone, and the side-chains of both light and heavy chain CDR1, CDR2, CDR3 are colored green, cyan, blue, yellow, orange and magenta, respectively. Views on left and right are identical but for a 90° rotation around a vertical axis. (D) Superposition of MK-5890-bound CD27 with CD27 bound to antibody M2177 (left two cartoons) or H2191 (center two cartoons) or CD27 in its CD70-bound form (PDB 7KX0). The CD27 antigen is represented as a ribbon. CD27 bound to MK-5890 is colored in gray and the residues involved in the epitope are colored in black. Its N-termini and C-termini are marked with a sphere and labeled, and the disulfide bridges are shown with green bonds. The structures of the antigen in the other costructures with Fabs are also shown as ribbons after alignment, but are colored according to the distance between Cα's using the costructure with MK-5890 as reference; the coloring forms a gradient from yellow to red and red to magenta for distances from 0 to 2.5 Å and 2.5 to 5.0 Å, respectively. The left and right panel for each of M2177, H2191, and 7KX0 is the same structure depicted with a rotation of 90° around a vertical axis. The orientations are identical for the three left panels of M2177, H2191, and 7KX0 as well as for the three right panels. (E) Comparison of the CD27 epitopes of MK-5890 and CD70. MK-5890 is shown as in figure 1B, with the same color conventions. The structure of the CD70-CD27 complex is moved as a rigid-body to superpose one copy of the antigen in the CD70-CD27 trimer with the MK-5890-bound CD27. For simplification, only the two CD70 molecules in contact with the CD27 structure of reference are shown, both as cartoons, one colored pink and the other magenta. MFI, mean fluorescence intensity; CH, constant heavy; CL, constant light; VH, variable heavy; VL, variable light.

5TL5) or H2191 (PDB 5TLK).[23] In addition, comparing the MK-5890:CD27 and CD27:CD70 structures[22] explains how CD70 can still partially bind when MK-5890 is bound (figure 1E).

Agonist activity

To evaluate antibody-mediated activation of CD27, induction of NF-κB by soluble anti-CD27 antibodies was measured in 293FT luciferase reporter cell lines expressing human or rhesus monkey CD27. MK-5890 induced NF-κB activation in soluble form, while varlilumab had no activity (figure 2A). MK-5890 had similar potency in rhesus monkey and human CD27 assays (EC_{50} of 0.29±0.16 nM and 2.22±2.17 nM, respectively).

Next, the ability of these antibodies to costimulate activation of primary human CD8+ T cells which were suboptimally stimulated with anti-CD3 and anti-CD28 mAbs was assessed. In the presence of soluble MK-5890, the proportion of human CD8+ T cells expressing the activation markers CD25 and CD69 increased 2.13±0.93 fold compared with the hIgG1 isotype control (figure 2B), while varlilumab did not show costimulatory activity in soluble form. MK-5890 and varlilumab had similar enhanced activity when coated onto beads (figure 2C). MK-5890 was not able to enhance T-cell proliferation in the absence of anti-CD3/anti-CD28 stimulation (online supplemental additional file 3, figure 1), indicating that it did not act as a so-called superagonist.[24] A human IgG2 version of MK-5890 had similar activity in this assay, confirming the agonist activity is not dependent on FcγR-mediated cross-linking in the assay (online supplemental additional file 3, figure 2).

The ability of MK-5890 to stimulate production of IFNγ by human tumor-infiltrating lymphocytes (TIL) in the presence of CD3 stimulation was evaluated using primary human tumor cultures. Mixed cell populations from NSCLC were used in these experiments to mimic the tumor microenvironment. MK-5890 enhanced anti-CD3-induced IFNγ production in the tumor cultures in a dose-dependent manner (figure 2D), while varlilumab did not. Because these cultures include cells that express FcγRs that may bind to and cross-link IgG1 antibodies, an Fc mutant (D265A) mouse IgG1 chimera of the parental mouse clone hCD27.131A and an hIgG2 version of MK-5890 were tested. Neither the D265A Fc mutant that does not bind to FcγR (figure 2D), nor the hIgG2 that weakly binds to FcγR (online supplemental additional file 3, figure 3) costimulated IFNγ production in this assay.

Confirmation that MK-5890 has costimulatory agonist activity on rhesus monkey cells was tested using CD4+CD25- T cells suboptimally stimulated with anti-CD3 and anti-CD28 mAbs. The presence of cross-linked, bead-bound MK-5890 led to a comparable increase in the activation markers CD25 and CD69 on both human and rhesus monkey CD4+CD25- T cells with EC_{50} of 0.13±0.03 µL beads/well and 0.14±0.02 µL beads/well, respectively (figure 2E).

Efficacy in syngeneic mouse tumor models

Though MK-5890 differentiates from varlilumab in agonist activity assays in vitro, it remained unclear whether this would translate to an anti-tumor efficacy advantage in vivo. Because MK-5890 does not bind to mouse CD27, huCD27 KI mice were generated in which the DNA sequences encoding the extracellular domain of mouse CD27 gene were replaced by those encoding the equivalent human domain. The mouse syngeneic MC38 tumor model in huCD27KI mice was selected for monotherapy efficacy based on its responsiveness to other T cell immunotherapies.[25] Both MK-5890 and varlilumab induced significant anti-tumor efficacy compared with isotype control ($p<0.001$ and $p<0.05$, respectively) in this model, though MK-5890 was significantly more effective than varlilumab ($p<0.05$) (figure 3A). MK-5890's efficacy was dependent on its interaction with FcγR, since it was lost when MK-5890 was engineered onto a human IgG2 Fc, either wild-type or with an N297A mutation to further reduce FcγR interactions. Consistent with earlier reports,[24] a similar loss of efficacy was observed with chimeric Fc mutant varlilumab antibody (data not shown). The mouse syngeneic MB49 tumor model was selected for testing combination therapy due to its minimal responsiveness to treatment with anti-PD-1.[25] In this model, MK-5890, varlilumab, or muDX400 displayed no significant monotherapy efficacy relative to isotype control, while the combination of MK-5890 or varlilumab with muDX400 resulted in significant efficacy relative to isotype control ($p<0.001$ and $p<0.005$, respectively). However, only the combination of MK-5890 with muDX400 resulted in significant efficacy relative to either monotherapy ($p<0.01$) (figure 3B). Such combined efficacy was not observed when the hIgG2 isotype of MK-5890 was used.

Impact on circulating lymphocytes and chemokines in vivo

The impact of MK-5890 on T-cell subpopulations in blood and tumor in the huCD27 KI syngeneic mouse MC38 tumor model was assessed by flow cytometry on day 10 after start of dosing. Administration of MK-5890 two times a week for three doses resulted in a significant decrease in total numbers of CD4+ T cell, CD8+ T cell, and CD4+FoxP3+ regulatory T-cell subsets in the blood on day 10 after the first dose, while no significant change was observed in the number of any T-cell subpopulation per mg of tissue in the tumor (figure 4A). The ratio of CD8+ to regulatory T cells was also decreased in the blood but not in the tumor. Anti-GITR antibody DTA-1 control resulted in a large, 115-fold decrease in Treg in the tumor as expected. The T cell changes in blood were isotype-dependent as they were not seen after dosing with MK-5890 hIgG2 isotype. A similar pattern was observed for a mouse IgG2a version of MK-5890 (hCD27.131A-mIgG2a; online supplemental additional file 4, figure 1), though a threefold reduction of Treg in the tumor compared with isotype control did reach significance. Comparable antitumor efficacy was found for hCD27.131A grafted onto mIgG1 and mIgG2a isotypes in the huCD27KI MC38 tumor model indicating

Figure 2: MK-5890 agonist activity in vitro

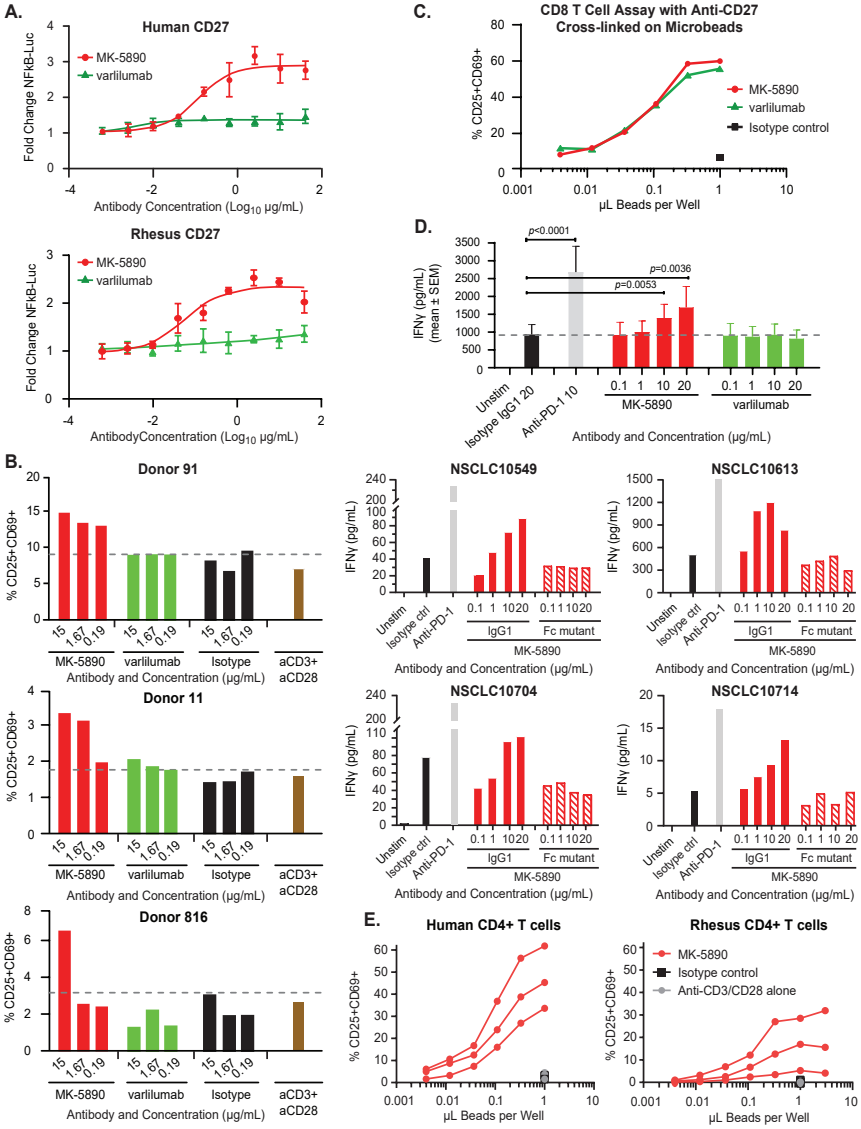

Figure 2 MK-5890 agonist activity in vitro. (A) Induction of CD27 signaling by soluble anti-CD27 mAbs was measured using 293FT-NF-κB-luciferase reporter cells transiently transfected with human or rhesus monkey CD27. Luciferase activity was assayed with Bright Glo and fold change compared with untreated cells was used for determination of EC_{50}. Error bars represent SD of triplicate wells. Data are representative of six experiments. (B) Naïve human CD8+ T cells were activated with a suboptimal concentration of anti-CD3 mAb and costimulated with anti-CD28 mAb in the presence of 15, 1.67, or 0.19 µg/mL anti-CD27 or isotype control mAbs and cultured for 3 days. Next, activated CD25+CD69+ CD8+ T cells were detected by flow cytometry. Representative flow cytometry plots can be found in online supplemental additional file 1. (C) Naïve human CD8+ T cells were activated with a suboptimal concentration of anti-CD3 mAb and costimulated with anti-CD28 mAb in the presence of variable amounts of Epoxy M-450 Dynabeads coupled to anti-CD27 mAbs or isotype control and cultured for 3 days. Next, activated CD25+CD69+ CD8+ T cells were detected by flow cytometry. (D) Human NSCLC tumor tissues obtained from surgical resections were digested into single cell suspensions using collagenase type I and DNase I. Enriched live cells containing a mixture of various cell types from the tumor were treated with 10 ng/mL anti-CD3 mAb combined with the indicated concentrations of MK-5890, anti-PD-1 antibody pembrolizumab, or isotype control (Top panel, n=13). Interferon gamma (IFNγ) in supernatants was measured on day 6. P values for comparison between treatment groups and the isotype control group were determined by non-parametric Dunn's multiple comparisons test. In a similar assay set-up, MK-5890 was compared with a chimeric mIgG1 D265A Fc mutant version of MK-5890 mouse clone hCD27.131A, or human IgG1 isotype control (bottom panel, four donors shown). (E) Naïve human or rhesus monkey CD4+CD25- T cells from three individual donors each were activated with a suboptimal concentration of anti-CD3 mAb and costimulated with anti-CD28 mAb in the presence or absence of variable amounts of Epoxy M-450 Dynabeads coupled to MK-5890 or isotype control and cultured for 3 days. Next, activated CD25+CD69+ CD4+ T cells were detected by flow cytometry. The EC_{50} was calculated based on the µL of beads per well. NSCLC, non-small cell lung cancer.

Figure 3: Anti-tumor efficacy in human CD27 knock-in mouse syngeneic tumor models

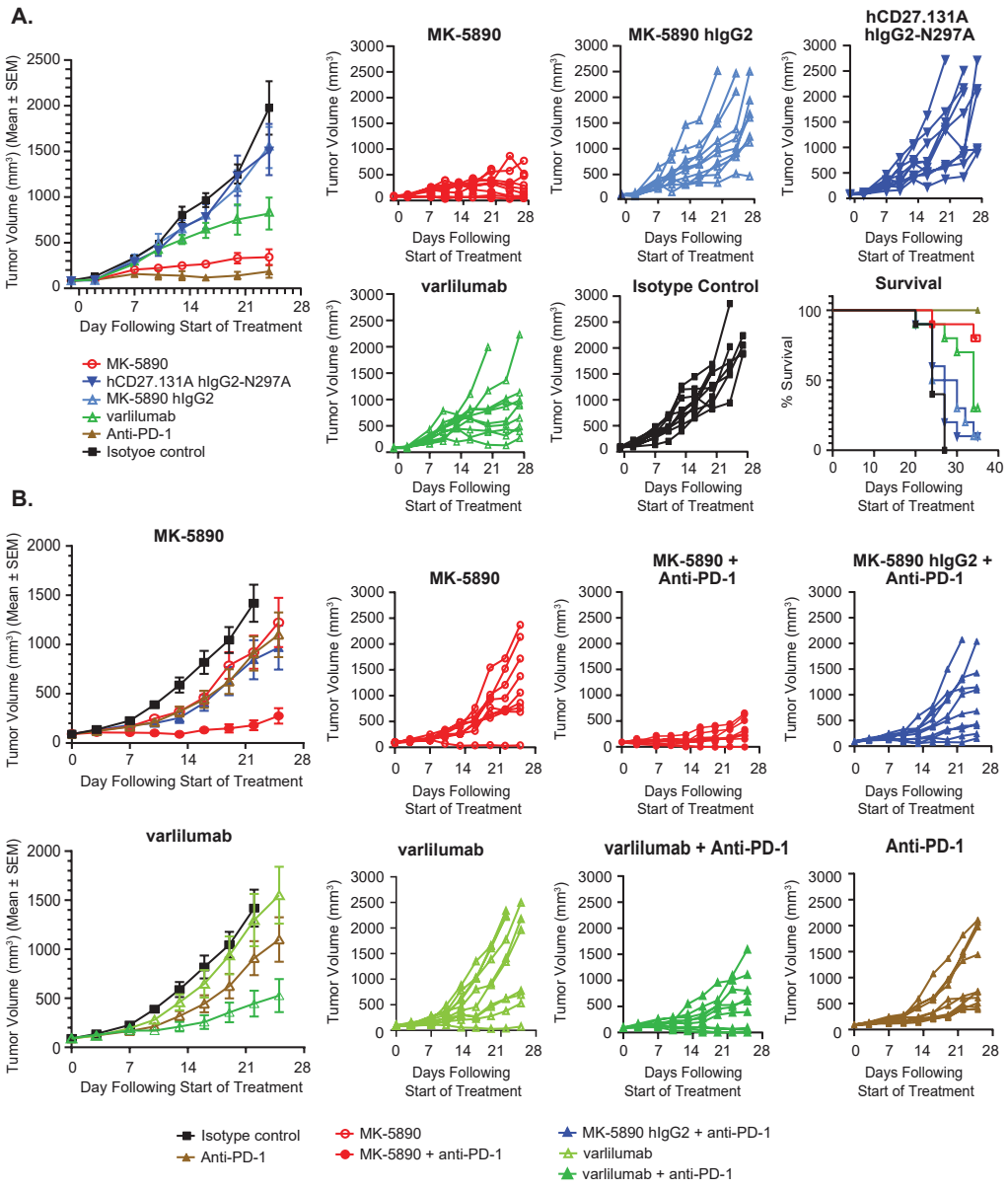

Figure 3 Antitumor efficacy in human CD27 knock-in mouse syngeneic tumor models. (A) MC38 mouse colon adenocarcinoma cells were implanted s.c. into immunocompetent huCD27 KI mice. Animals were assigned to treatment groups and dosing was started 6 days after implant when the mean starting tumor volume reached 88 mm^3. 5 mg/kg MK-5890 (hIgG1), MK-5890 hIgG2, hCD27.131A hIgG2-N297A, varlilumab or anti-infectious bursal disease virus (IBDV) VP2-4-3_GV mouse IgG2a isotype control mAb were administered on Days 0, 3, 7, 10, 14, 17, and 21. 5 mg/kg anti-PD-1 muDX400 (mIgG1 D265A) was administered on days 0, 3, 7, and 10. Left panel shows mean tumor volume+/-SEM; right panels show individual animal tumor volumes and survival curves, with end of survival defined by tumor volume exceeding 2000 mm^3, severe tumor ulceration, or humane endpoints. n=10/group. (B) MB49 mouse urothelial cells were implanted subcutaneously into immunocompetent huCD27 KI mice. Animals were assigned into treatment groups and dosing started 7 days after implant when the mean starting tumor volume reached 91 mm^3. Animals were dosed with 5 mg/kg MK-5890, MK-5890 hIgG2, varlilumab or anti-PD-1 muDX400 alone, or with a combination of 5 mg/kg anti-PD-1 muDX400 with either 5 mg/kg MK-5890, MK-5890 hIgG2, or varlilumab, or with 5 mg/kg each of anti-IBDV VP2-4-3_GV mouse IgG2a and anti-respiratory syncitial virus mIgG1 D265A isotype control mAbs. MK-5890, MK-5890 hIgG2, varlilumab and isotype control mAbs were administered i.p. on Days 0, 4, 7, 11, 14, and 18. Anti-PD-1 muDX400 was administered intraperitoneally on days 0, 7, 14, and 21. n=10/group.

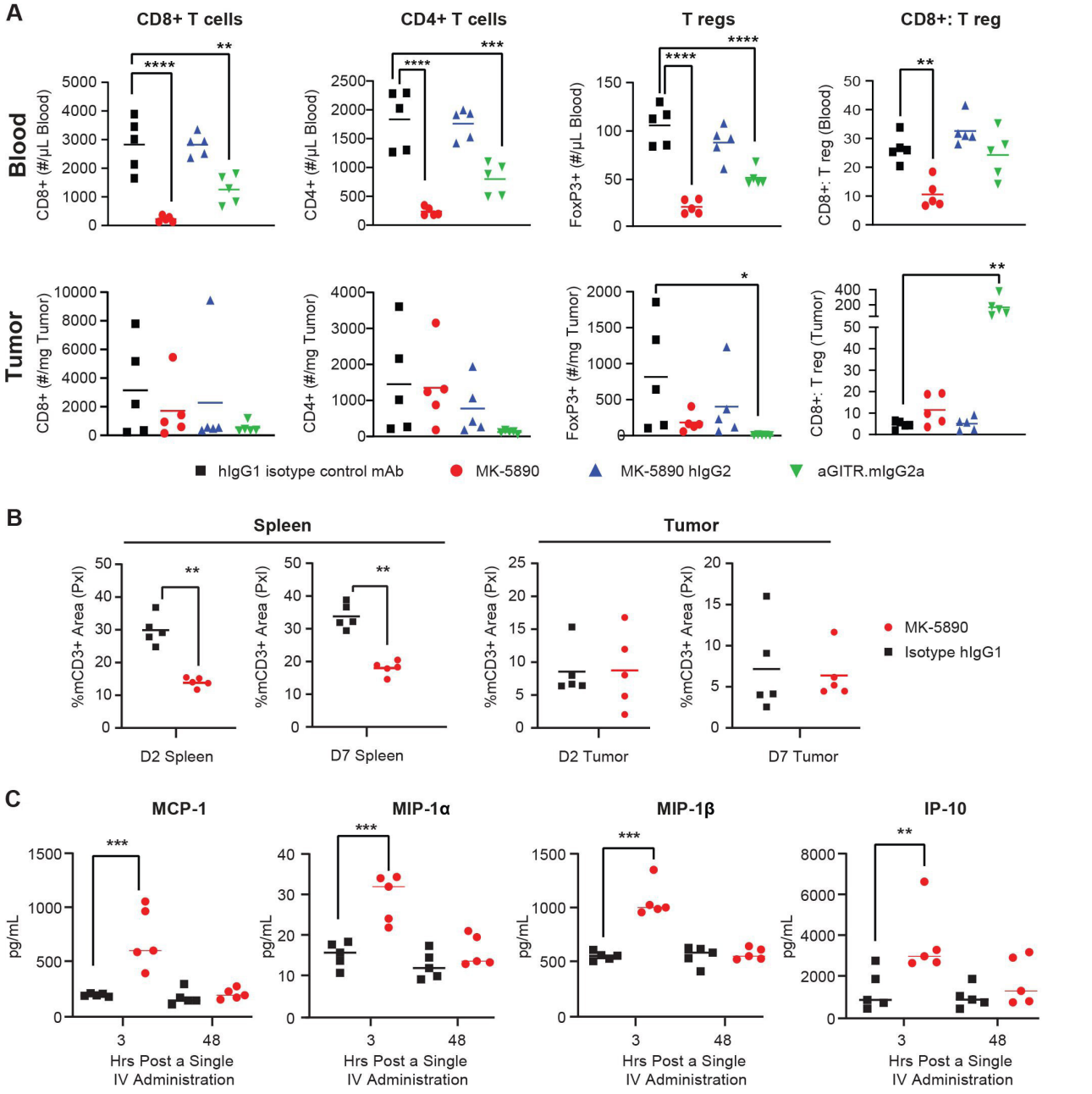

Figure 4 Pharmacodynamic effects in human CD27 knock-in mouse MC38 tumor model. MC38 cells were implanted s.c. into immunocompetent huCD27 KI mice. Animals were assigned to treatment groups and dosing was started when the mean starting tumor volume reached 83–86 mm^3. (A) 5 mg/kg of MK-5890 (hIgG1), MK-5890 hIgG2, or anti-RSV human immunoglobulin G, subclass 1 (hIgG1) isotype control mAb were administered intraperitoneally on days 0, 3, and 7 for a total of three doses. A 5 mg/kg murinized anti-GITR antibody mDTA-1 was administered subcutaneously on day 0 (a previously established efficacious regimen in the MC38 tumor model). Blood and tumors were extracted on study day 10 and processed for analysis of T cell subpopulations by flow cytometry as described in online supplemental additional file 1. Total numbers of CD4+ T cells, CD8+ T cells, FoxP3+ T regulatory cells per microliter of blood (top panel) or per mg of tumor (lower panel) and CD8+:Treg ratio on study day 10 are shown. Data are presented by treatment group for individual animals as well as by group mean. *p≤0.05, **p≤0.01, ****p≤0.0001, respectively, for comparison between isotype control and anti-CD27 mAb treatment groups by one-way analysis of variance with Dunnett's multiple comparisons test (GraphPad Prism). Only comparisons with significant differences are shown. (B) 5 mg/kg MK-5890 or isotype control was administered intravenous on day 0. Tumors were collected on day 2 and day 7, fixed in formalin and embedded in paraffin. 5 micron sections were stained for CD3+ T cells. Whole slide images were acquired at ×20 resolution with Aperio ScanScope brightfield scanner and analyzed using a customized Definiens Developer 2.6 algorithm. CD3 stain area was normalized against nuclear stain and expressed as per cent area. (C) 5 mg/kg of MK-5890 or isotype control mAb was administered intravenous and terminal blood was collected after 3 and 48 hours. Serum was analyzed by electrochemiluminescence using a custom chemokine U-plex panel (Mesoscale) according to manufacturer's instructions. **p<0.01, ***p<0.001 and, respectively, as analyzed by the non-parametric unpaired Mann-Whitney U t-test for (B, C). RSV, respiratory syncitial virus.

that induced T cell costimulation rather than the small decrease in Treg is driving the observed antitumor efficacy (online supplemental additional file 4, figure 2).

Immunohistochemical analysis of CD3+ T cells in the spleen and MC-38 tumor showed a 50% reduction of splenic T cells beginning at 2 days after the first dose. In the tumors of these animals, no change in the density of T cells was observed by IHC after MK-5890 treatment (figure 4B).

We next investigated whether MK-5890-mediated changes in circulating chemokines and cytokines could be detected. Serum was evaluated 3 and 48 hours after a single intravenous dose of antibody in the same tumor model. Transient increases in MCP-1, MIP-1α, MIP-1β and IP-10 were observed 3 hours after dosing MK-5890 (figure 4C). With the exception of elevated MIP2, no changes were observed for the other cytokines tested (TNFα, IFNγ, IL6, IL16, and KC/GRO).

Assessment of MK-5890 safety, pharmacokinetics, and pharmacodynamic markers in rhesus monkey

MK-5890 administered intravenous to rhesus monkeys once weekly at doses of 0.1 mg/kg, 3 mg/kg, or 30 mg/kg/week in a 4-week toxicology study was well tolerated. Systemic exposure to MK-5890 was associated with receptor occupancy at all doses, as measured in a target engagement assay, confirming the pharmacodynamic activity of MK-5890. Systemic exposure to MK-5890 increased with increasing doses (figure 5A, table 2) and was independent of sex. Mean $AUC_{0\text{-}168h}$ values were greater than dose proportional across doses, and C_{max} values were approximately dose proportional from 0.1 mg/kg/week to 3 mg/kg/week and greater than dose proportional from 3 mg/kg/week to 30 mg/kg/week. Following repeat weekly dosing, anti-MK-5890 antibodies were detected in a few animals across all dose groups. Animals with anti-MK-5890 antibodies generally showed corresponding increased elimination of serum MK-5890 and decreased CD27 receptor occupancy.

MK-5890-related findings were limited to changes in hematology, serum chemistry and cytokine parameters with no changes in histomorphology. Slightly increased IL-6 levels (>3 times the highest pretest and control values) were observed transiently on study day 1 at the 0.1 mg/kg and 3 mg/kg doses. Very slight decreases in white blood cell and lymphocyte counts relative to concurrent vehicle controls were observed across all dose groups and were associated with decreases in subsets of lymphocytes (including total T cells, CD4+ T cells, CD8+ T cells, NKT cells and NK cells) as identified by immunophenotyping. MK-5890 showed no apparent effect on B cell or regulatory T cell numbers in peripheral blood and no corresponding histomorphologic changes were observed in lymphoid tissues. At the end of the treatment free period, a complete recovery of the lymphocyte counts was observed in all animals in all dose groups (except for one female at 3 mg/kg/week).

In a preceding single dose PK/PD study in rhesus monkeys (online supplemental additional file 1), IP-10, MCP-1, MIP-1α and MIP-1β chemokines were shown to be transiently elevated in serum, while Eotaxin-3, TARC, IL-8, MDC, MCP-4 were not changed (figure 5C).

Assessment of pharmacokinetics and pharmacodynamic markers in a phase 1 dose-escalation study

MK-5890 was tested in a first-in-human study in patients with advanced solid tumors alone (dose range, 2–700 mg) or with pembrolizumab (fixed dose, of 200 mg) as described by Shapira-Frommer *et al*.[26] Available PK data from participants treated with escalating doses of MK-5890 when given as monotherapy or in combination with pembrolizumab showed that serum MK-5890 exposures and CD27 receptor occupancy on circulating T cells increased in a dose-dependent manner. These data corroborated with observations in the non-human primate study. PK profiles of MK-5890 exposures suggest that target-mediated clearance of MK-5890 is saturated at the 200 mg and 700 mg doses (figure 5B, table 2). Decreases in circulating T cells were observed by immunophenotyping consistent with data in rhesus monkeys, but no clinically significant lymphopenia events were observed in the dose-escalation study. As observed in studies in mouse and in rhesus monkey MCP-1, MIP-1α and MIP-1β chemokines were transiently elevated (figure 5D). Data for IP-10 were not interpretable due to limited data collected.

DISCUSSION

MK-5890 is a novel anti-human CD27 agonist humanized IgG1 antibody that was identified and selected by virtue of its ability to activate the human CD27 receptor in an NF-κB luciferase reporter cell line assay without requirement for clustering via Fc-FcγR interaction. This unique activity was confirmed using purified CD8+ T cells, where MK-5890 costimulates T-cell activation, in the presence of TCR and CD28 (co)stimulation. This differentiates MK-5890 from varlilumab, a human anti-CD27 antibody that can only costimulate CD4+ or CD8+ T cells in vitro when crosslinked.[15] The costimulatory effect of MK-5890 on purified CD8+ T cells was further enhanced when the antibody was coated on beads, suggesting that in a physiological setting where FcγRs are present, Fc-mediated crosslinking may be important for optimal activity of MK-5890.

TNFR trimers formed on transmembrane ligand binding are known to aggregate in the plane of the membrane into higher order multimers, which is important for initiation of signal transduction.[27] We show that MK-5890 binds to the N-terminal region of the CRD1 domain, which is the most rigid structure in the TNFR family. Therefore, MK-5890 binding to CD27 is not likely to induce a conformational change in the CD27 monomer, but more likely induces CD27 oligomerization. The antigen flexibility, through the Fab elbow angle and the hinge between Fc and Fabs, may facilitate such

Figure 5: Single dose pharmacokinetics and pharmacodynamics in rhesus monkeys and in Phase 1 dose escalation clinical study

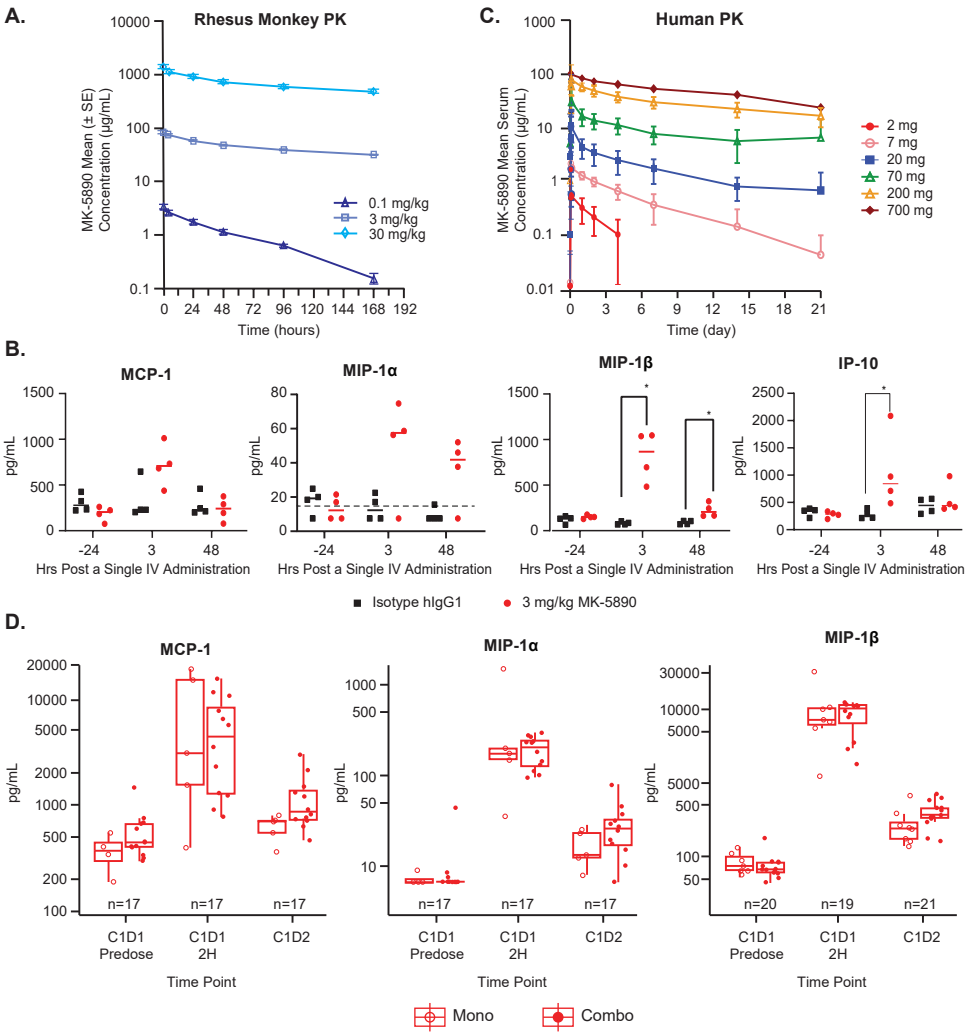

Figure 5 Serum drug and chemokine concentrations after single dose administration of MK-5890 in rhesus monkeys and in a Phase one dose escalation clinical study. (A) Summary mean (± SE) serum MK-5890 concentrations (µg/mL) in female and male rhesus monkeys following a single intravenous bolus injection of 0 (vehicle control), 0.1, 3, or 30 mg/kg MK-5890 on study day 1. (B) 3 mg/kg of MK-5890 or anti-RSV human immunoglobulin G, subclass 1 (hIgG1) isotype control mAb were administered intravenously on Day 0 to male rhesus monkeys. Serum samples from blood collected 24 hours predose, 3 hours and 48 hours postdose were analyzed by electrochemiluminescence using a non-human primate chemokine V-plex panel (Mesoscale) according to manufacturer's instructions. Data are presented by treatment group for individual animals as well as by group median. *p≤0.05 for comparison between isotype control and MK-5890 treatment groups by non-parametric Mann-Whitney U t-test (GraphPad Prism). Only comparisons with significant differences are shown. (C) Arithmetic mean (±SD) plasma concentration of MK-5890 versus time from the monotherapy (MK-5890 alone) and combination (MK-5890+pembrolizumab) arms in subjects from the ongoing MK-5890–001 trial @ 2, 7, 20, 70, 200 and 700 mg. (D) 200 mg MK-5890 as monotherapy (open symbols) or in combination with pembrolizumab (closed symbols) were infused on cycle 1 day 1 (C1D1) to patients with advanced solid tumors. Serum samples from blood collected predose, 2 hours postdose, and cycle 1 day 2 (C1D2) were analyzed using fit-for-purpose validated immunoassays to measure the abundance of these cytokines in serum. Data are presented by individual participants in boxplots. For MCP-1 and MIP-1α, n=6 from monotherapy and n=14 from combination therapy; for MIP-1β, n=8 from monotherapy and n=14 from combination therapy. Data for IP-10 is not shown as it was uninterpretable due to limited data collected. RSV, respiratory syncitial virus.

Table 2 Pharmacokinetic characteristics of MK-5890 in a Rhesus monkey toxicology study and in a Ph1 clinical study

Summary mean (±SE) pharmacokinetic parameters in Rhesus monkey after single bolus IV dose of MK-5890 in a toxicology study				Summary geometric mean (%GCV) serum pharmacokinetic parameters after single IV infusion* of MK-5890 in a Ph1 clinical study			
Dose (mg/kg)	Cmax (µg/mL)	Tmax (hour)	$AUC_{0–168\ hours}$ (hour*µg/mL)	Dose (mg)	Cmax (µg/mL)	Tmax† (hour)	$AUC_{0–21\ days}$ (day×µg/mL)
0.1	3.27±0.278	0.25±0.0	163±10.7	2	1.15 (175.3)	1.50 (1.50–2.00)	1.33 (88.7)
3	84.1±4.10	0.63±0.38	7540±200	7	2.18 (40.1)	1.50 (1.50–2.00)	7.80 (53.6)
30	1330±84.7	0.25±0.0	114000±7050	20	6.70 (51.6)	2.00 (1.50–2.00)	31.5 (93.2)
				70	21.6 (22.0)	1.50 (1.50–2.00)	154 (9.2)
				200	67.8 (23.1)	1.50 (1.50–2.00)	527 (28.7)
				700	105 (8.7)	1.50 (1.50–1.50)	1070 (0.1)

*MK-5890 delivered by intravenous infusion in human participants over a duration of 60–90 min.
†Median (min-max).
%GCV, % geometric coefficient of variation.

oligomerization. In fact, induction of oligomerization was described for hCD27.15, an antibody that overlaps in binding to CD27 with MK-5890.[16] The orientation of the antigen relative to the Fab is important for bringing two CD27 molecules into proximity. The slanted, external-facing orientation of MK-5890 on CD27 largely allows the interaction with CD70, thereby explaining its partial blocking of the CD70 interaction.

Oligomerization as a mechanism of action of MK-5890 is further supported by the observed Fc-mediated amplification of CD27 activation induced by MK-5890. In a costimulation assay using single cell suspensions of primary human NSCLC tumors, which contain FcγR-bearing myeloid cells that express CD80 and CD86 in addition to TIL and tumor cells, the MK-5890 human IgG1 isotype enhanced IFNγ production, but MK-5890 with a D265A Fc mutation (no FcγR binding) did not. Similarly, the potent anti-tumor activity of MK-5890 in huCD27KI mouse subcutaneous tumor models was lost with isotypes that do not bind to FcγRs, consistent with what has been reported for varlilumab.[28] Therefore, enhancement of the intrinsic agonistic activity of MK-5890 through FcγR-mediated crosslinking appears to be important to drive an effective immune response in more complex in vitro or in vivo settings. MK-5890 consistently demonstrated stronger potency in TIL cultures and in vivo models compared with varlilumab, indicating that the differences in activity observed in reporter assays and purified CD8+ T cell assays are indeed relevant.

MK-5890 dosing resulted in decreased circulating CD4+ and CD8+ T cell numbers in huCD27KI mice. In rhesus monkey and human patients MK-5890 resulted in transient dose-dependent decreases in circulating total, CD4+ and CD8+ T lymphocytes, though to a much lesser degree than observed in mice. Moreover, this was not associated with significant lymphopenia and lymphocytes numbers returned to baseline when MK-5890 treatment was stopped. Previously, studies in CD70 transgenic mice showed that, depending on the cell type expressing transgenic CD70, chronic CD27/CD70 engagement in the context of T cell receptor triggering can enhance turnover of naïve T cells into terminally differentiated effector cells which migrate to tissues and are subject to CD95-mediated apoptosis.[29–34] Our and other studies[16 35] assessed the effect of CD27 activation in a fully developed immune system using antibody treatment with no evidence of immunodeficiency, making the mechanisms observed on chronic CD27 stimulation in CD70 transgenic mice less likely to explain the observed reduction in systemic lymphocytes.

Wasiuk *et al*[35] suggested Treg death, either activation-induced or antibody-dependent cellular cytotoxicity/phagocytosis as the mechanism for antitumor efficacy in mouse subcutaneous tumor models. However, they also observed greater anti-tumor effects from pretreatment with varlilumab (1F5) compared with PC.61 anti-CD25 antibody (which resulted in similar Treg depletion), indicating a role for CD27 agonism in varlilumab tumor growth inhibition. In the case of MK-5890, CD4+ and CD8+ T cells were not decreased in the tumor, though Tregs did show an approximate threefold decrease. This decrease in intratumoral Tregs was rather minimal as compared with the observed >100 fold anti-GITR DTA-1-mediated Treg depletion. Furthermore, varlilumab, which binds to CD27 with higher affinity compared with MK-5890 is less efficacious.[17] Together with the observed similar anti-tumor activity for MK-5890 grafted onto mIgG2a and mIgG1 isotypes (strongly depleting vs minimally depleting isotypes, respectively), the data collectively points to a role for MK-5890-mediated CD27 activation during tumor rejection rather than simply intratumoral Treg depletion.

MK-5890 dosing induced a rapid, transient increase in circulating chemokines IP-10, MCP-1, MIP-1α, and MIP-1β within 3 hours. Similarly, Turaj *et al* demonstrated that CD27 costimulation of activated CD8+ T cells and NK cells induced the secretion of MIP-1α, MIP-1β, and RANTES, thereby potentially attracting lymphocytes and

myeloid cells.[36] The chemokines that were induced by MK-5890 are hallmarks of T-cell activation, IFNγ production and/or CD4+ T cell/DC interaction[37] and thus indicative of MK-5890 induced CD27 activation across all three species. Finally, the observed reduction of tumor Tregs might be due to increased T cell activation, as suggested for bempegaldesleukin where IFNγ from T cell activation results in a reduced number of intratumoral Tregs.[38]

Recent insights demonstrate that so-called predysfunctional T cells are the target of PD-1 blockade. We have recently proposed that these predysfunctional CD8+ T cells have lacked CD4+ T-cell help signals during priming[12] and are therefore incompletely differentiated into effective CTLs. Providing CD4+ T-cell help, or mimicking 'help' signals[39] in the presence of PD-1 blockade, is thought to result in reinvigoration of fully functional CTLs. Based on the similar costimulatory effect of MK-5890 and the anti-mouse CD27 antibodies that were used during these earlier studies,[9 13] we hypothesize that MK-5890-mediated CD27 costimulation mimics CD4+ T-cell help and therefore endows the CD8+ T cell with the optimal anti-tumor activities and generates CTL memory.

MK-5890 was well tolerated and showed signs of activity in pharmacokinetic and toxicity studies in rhesus monkeys. In both rhesus monkey and in the phase 1 clinical dose escalation study, MK-5890 exposure and CD27 receptor occupancy increased on circulating T cells in a dose-dependent manner. Currently, clinical evaluation of MK-5890 is ongoing in various combinations in solid tumors (phase 1 NCT03396445; phase 2, NCT04165096 and NCT04165070).

CONCLUSIONS

Here, we characterized MK-5890, a CD27 agonist antibody that can activate CD27 signaling without the need for antibody crosslinking and has potent antitumor activity in preclinical models both as monotherapy and in combination with PD-1 checkpoint inhibition. Clinical translation of CD27 agonism is suggested by pharmacodynamic readouts that are consistent between preclinical models and patients with cancer.

Author affiliations
[1]BioNovion/Aduro Biotech Europe, Oss, The Netherlands
[2]Discovery, Preclinical and Translational Medicine, Merck & Co Inc, Kenilworth, New Jersey, USA
[3]Discovery, Preclinical and Translational Medicine, Merck & Co Inc, South San Francisco, California, USA
[4]Division of Immunology, The Netherlands Cancer Institute, Amsterdam, The Netherlands
[5]Clinical Development, Merck & Co Inc, Rahway, New Jersey, USA
[6]Discovery, Preclinical and Translational Medicine, Merck & Co Inc, West Point, Pennsylvania, USA
[7]Process Research and Development, Merck & Co Inc, Kenilworth, New Jersey, USA

Acknowledgements The authors would like to thank Xuemei Zhao, Allen Wong, and Lucia Franco-Dilone from Translational Molecular Biomarkers, Merck & Co., Inc., Rahway, NJ, USA for the acquisition and analysis of cytokines in the first-in-human clinical study.

Contributors AMB, AvE, DR, EC, HVE, JBa, JKC, JBo, JWa, LG, RW, ST, and SM contributed to conception, design or planning of the studies. AMB, ABr, ABe, DM, DG, DLH, DR, EdV, IL, JBa, JW, JK, JS-V, LF-D, LD-E, MG, MH, NB, RW, SM and WP contributed to acquisition of the data. AMB, ABr, ABe, ABo, DM, DLH, DR, EC, EdV, HVE, IL, JBo, JWo, JWa, JS-V, LG, LF-D, LD-E, MG, MH, NB, RW, ST and SM contributed to analysis of the data. AMB, DR, EC, HVE, JBo, JKC, JWa, KD, LG, LF-D, LD-E, MH, RW, ST and SM contributed to interpretation of the results. AMB, DLH, HVE, JWo, JWa, LG, RW and ST drafted the manuscript. AMB, AvE, ABr, ABe, ABo, DM, DG, DLH, DR, EC, EdV, HVE, IL, JBa, JKC, JBa, JK, JWa, JS-V, KD, LG, LF-D, LD-E, MG, MH, NB, ST, SM and WP critically reviewed or revised the manuscript. AMB and HVE are responsible for the overall content as guarantors.

Funding Funding for this research was provided by Merck Sharp & Dohme LLC, a subsidiary of Merck & Co, Rahway, New Jersey, USA. Funding for a portion of the research done at The Netherlands Cancer Institute, Amsterdam, The Netherlands and at BioNovion/Aduro Biotech Europe, Oss, The Netherlands was funded by the T3-112 and T3-504 grant from Top Institute Pharma, Leiden, the Netherlands was provided by Top Institute Pharma grants T3-112 and T3-504.

Competing interests TOF, JWo, SM, VJ, DR, WP, DG, YY, JBa, DM, YZ, RW, ST, EC SS, KD, JKC, LF-D and AMB are or were employed by Merck Sharp & Dohme LLC, a subsidiary of Merck & Co. Inc., Rahway, NJ, USA and may own stock in Merck & Co. Inc., Rahway, NJ, USA. ABr, DLH, HVE, JK, LG, LD-E were employed by BioNovion/Aduro Biotech Europe, Kloosterstraat 9, 5349 AB, Oss, The Netherlands and have stock that has since been converted to Chinook Therapeutics Inc. stock. AMB, JKC, VJ, LF-D, SS, JWo, HVE, AvE, LG, TOF and WP are authors on a related patent which is assigned to Merck Sharp & Dohme LLC, Rahway, NJ (US); Merck Sharp & Dohme B.V., Haarlem (NL).

Patient consent for publication Not applicable.

Provenance and peer review Not commissioned; externally peer reviewed.

Data availability statement Data are available in a public, open access repository. All data relevant to the study are included in the article or uploaded as online supplemental information. X-ray crystal structure factors and coordinates files have been deposited for public access in the Protein Data Bank (PDB, http://www.rcsb.org) under the code 8DS5.

ORCID iD
Amy M Beebe http://orcid.org/0000-0002-8892-0607

REFERENCES

1 Wajant H. Therapeutic targeting of CD70 and CD27. *Expert Opin Ther Targets* 2016;20:959–73.
2 Buchan SL, Rogel A, Al-Shamkhani A. The immunobiology of CD27 and OX40 and their potential as targets for cancer immunotherapy. *Blood* 2018;131:39–48.
3 Goodwin RG, Alderson MR, Smith CA, *et al*. Molecular and biological characterization of a ligand for CD27 defines a new family of cytokines with homology to tumor necrosis factor. *Cell* 1993;73:447–56.
4 Hendriks J, Xiao Y, Borst J. CD27 promotes survival of activated T cells and complements CD28 in generation and establishment of the effector T cell pool. *J Exp Med* 2003;198:1369–80.
5 Peperzak V, Xiao Y, Veraar EAM, *et al*. CD27 sustains survival of CTLs in virus-infected nonlymphoid tissue in mice by inducing autocrine IL-2 production. *J Clin Invest* 2010;120:168–78.

6 Soares H, Waechter H, Glaichenhaus N, *et al*. A subset of dendritic cells induces CD4+ T cells to produce IFN-gamma by an IL-12-independent but CD70-dependent mechanism in vivo. *J Exp Med* 2007;204:1095–106.
7 Xiao Y, Peperzak V, Keller AM, *et al*. CD27 instructs CD4+ T cells to provide help for the memory CD8+ T cell response after protein immunization. *J Immunol* 2008;181:1071–82.
8 van de Ven K, Borst J. Targeting the T-cell co-stimulatory CD27/CD70 pathway in cancer immunotherapy: rationale and potential. *Immunotherapy* 2015;7:655–67.
9 Ahrends T, Spanjaard A, Pilzecker B, *et al*. $CD4^+$ T cell help confers a cytotoxic T cell effector program including coinhibitory receptor downregulation and increased tissue invasiveness. *Immunity* 2017;47:848–61.
10 Bullock TNJ, Yagita H. Induction of CD70 on dendritic cells through CD40 or TLR stimulation contributes to the development of CD8+ T cell responses in the absence of CD4+ T cells. *J Immunol* 2005;174:710–7.
11 Feau S, Garcia Z, Arens R, *et al*. The $CD4^+$ T-cell help signal is transmitted from APC to $CD8^+$ T-cells via CD27-CD70 interactions. *Nat Commun* 2012;3:948.
12 Busselaar J, Tian S, van Eenennaam H, *et al*. Helpless priming sends $CD8^+$ T cells on the road to exhaustion. *Front Immunol* 2020;11:592569.
13 Ahrends T, Bąbała N, Xiao Y, *et al*. CD27 agonism plus PD-1 blockade recapitulates CD4+ T-cell help in therapeutic anticancer vaccination. *Cancer Res* 2016;76:2921–31.
14 Sakanishi T, Yagita H. Anti-tumor effects of depleting and non-depleting anti-CD27 monoclonal antibodies in immune-competent mice. *Biochem Biophys Res Commun* 2010;393:829–35.
15 Vitale LA, He L-Z, Thomas LJ, *et al*. Development of a human monoclonal antibody for potential therapy of CD27-expressing lymphoma and leukemia. *Clin Cancer Res* 2012;18:3812–21.
16 Heckel F, Turaj AH, Fisher H, *et al*. Agonistic CD27 antibody potency is determined by epitope-dependent receptor clustering augmented through Fc-engineering. *Commun Biol* 2022;5:229.
17 Van Eenennaam H, Mulder WR, Borst JG. Agonistic antibody to CD27. United States patent US9527916B2 2016.
18 Beebe AM, Cheung JKJ, Juan V. Anti-CD27 antibodies. United States patent 20200131272 2017.
19 Keler T, Marsh HC, He L. Antibodies that bind human CD27 and uses thereof. United States patent US9169325B2 2015.
20 Lindauer A, Valiathan CR, Mehta K, *et al*. Translational pharmacokinetic/pharmacodynamic modeling of tumor growth inhibition supports dose-range selection of the anti-PD-1 antibody pembrolizumab. *CPT Pharmacometrics Syst Pharmacol* 2017;6:11–20.
21 Sukumar S, Wilson DC, Yu Y, *et al*. Characterization of MK-4166, a clinical agonistic antibody that targets human GITR and inhibits the generation and suppressive effects of T regulatory cells. *Cancer Res* 2017;77:4378–88.
22 Liu W, Maben Z, Wang C, *et al*. Structural delineation and phase-dependent activation of the costimulatory CD27:CD70 complex. *J Biol Chem* 2021;297:101102.
23 Obmolova G, Teplyakov A, Malia TJ, *et al*. Epitope-dependent mechanisms of CD27 neutralization revealed by X-ray crystallography. *Mol Immunol* 2017;83:92–9.
24 Tacke M, Hanke G, Hanke T, *et al*. CD28-mediated induction of proliferation in resting T cells in vitro and in vivo without engagement of the T cell receptor: evidence for functionally distinct forms of CD28. *Eur J Immunol* 1997;27:239–47.
25 Georgiev P, Muise ES, Linn DE, *et al*. Reverse translating molecular determinants of anti-programmed death 1 immunotherapy response in mouse syngeneic tumor models. *Mol Cancer Ther* 2022;21:427–39.
26 Shapira-Frommer R, van Dongen MGJ, Dobrenkov K. Phase 1 study of an anti-CD27 agonist as monotherapy and in combination with pembrolizumab in patients with advanced solid tumors. *J Immunother Cancer* 2020;8:A2.
27 Holler N, Tardivel A, Kovacsovics-Bankowski M, *et al*. Two adjacent trimeric Fas ligands are required for Fas signaling and formation of a death-inducing signaling complex. *Mol Cell Biol* 2003;23:1428–40.
28 He L-Z, Prostak N, Thomas LJ, *et al*. Agonist anti-human CD27 monoclonal antibody induces T cell activation and tumor immunity in human CD27-transgenic mice. *J Immunol* 2013;191:4174–83.
29 Nolte MA, van Olffen RW, van Gisbergen KPJM, *et al*. Timing and tuning of CD27-CD70 interactions: the impact of signal strength in setting the balance between adaptive responses and immunopathology. *Immunol Rev* 2009;229:216–31.
30 Arens R, Baars PA, Jak M, *et al*. Cutting edge: CD95 maintains effector T cell homeostasis in chronic immune activation. *J Immunol* 2005;174:5915–20.
31 Arens R, Tesselaar K, Baars PA, *et al*. Constitutive CD27/CD70 interaction induces expansion of effector-type T cells and results in IFNgamma-mediated B cell depletion. *Immunity* 2001;15:801–12.
32 Tesselaar K, Arens R, van Schijndel GMW, *et al*. Lethal T cell immunodeficiency induced by chronic costimulation via CD27-CD70 interactions. *Nat Immunol* 2003;4:49–54.
33 Keller AM, Schildknecht A, Xiao Y, *et al*. Expression of costimulatory ligand CD70 on steady-state dendritic cells breaks CD8+ T cell tolerance and permits effective immunity. *Immunity* 2008;29:934–46.
34 Nolte MA, Arens R, van Os R, *et al*. Immune activation modulates hematopoiesis through interactions between CD27 and CD70. *Nat Immunol* 2005;6:412–8.
35 Wasiuk A, Testa J, Weidlick J, *et al*. CD27-mediated regulatory T cell depletion and effector T cell costimulation both contribute to antitumor efficacy. *J Immunol* 2017;199:4110–23.
36 Turaj AH, Hussain K, Cox KL, *et al*. Antibody tumor targeting is enhanced by CD27 agonists through myeloid recruitment. *Cancer Cell* 2017;32:777–91.
37 Castellino F, Huang AY, Altan-Bonnet G, *et al*. Chemokines enhance immunity by guiding naive CD8+ T cells to sites of CD4+ T cell-dendritic cell interaction. *Nature* 2006;440:890–5.
38 Sharma M, Khong H, Fa'ak F, *et al*. Bempegaldesleukin selectively depletes intratumoral Tregs and potentiates T cell-mediated cancer therapy. *Nat Commun* 2020;11:661.
39 Borst J, Busselaar J, Bosma DMT, *et al*. Mechanism of action of PD-1 receptor/ligand targeted cancer immunotherapy. *Eur J Immunol* 2021;51:1911–20.